American Mineralogist, Volume 86, pages 1477–1482, 2001

Crystal structure analysis of synthetic $Ca_4Fe_{1.5}Al_{17.67}O_{32}$: A high-pressure, spinel-related phase

V. KAHLENBERG,[1,]* C.S.J. SHAW,[2] AND J.B. PARISE[3]

[1]Fachbereich Geowissenschaften (Kristallographie), Universität Bremen, Klagenfurter Str., D-28359 Bremen, Germany
[2]Bayerisches Geoinstitut, Universität Bayreuth, D-95440 Bayreuth, Germany
[3]Center for High Pressure Research, Department of Geosciences, State University of New York, Stony Brook, New York 11794-2100, U.S.A.

ABSTRACT

The compound $Ca_4Fe_{1.5}Al_{17.67}O_{32}$ was synthesized at 2.5 GPa and 1250 °C using a piston-cylinder apparatus. The crystal structure, determined from single-crystal X-ray diffraction data collected at 295 K (tetragonal, space group $I\bar{4}2d$, $a = 20.1847(14)$ Å, $c = 5.6203(6)$ Å, $V = 2289.83(3)$ Å^3, $Z = 4$) was refined to a final R-index of 0.024 for 1229 independent observed reflections and 130 parameters. The main building units comprising the compound are 11.8×7.2 Å wide spinel-type ribbons running parallel to [001], which are connected via corner-sharing (Fe,Al)O_6-octahedra. Additional linkage between the spinel units is provided by AlO_4-tetrahedra residing on the $\bar{4}$-axis as well as by Ca cations, in sevenfold coordination with oxygen attached to the spinel-like building units. Refinement of site occupancies reveals that the incorporation of Fe occurs at two of four octahedral and at two of three tetrahedral sites. Apparently, $Ca_4Fe_{1.5}Al_{17.67}O_{32}$ represents a new structure type exhibiting more pronounced structural modifications relative to the spinel aristotype compared with the so-called spinelloid structures. Furthermore, this synthetic compound contains Fe^{2+} in tetrahedral coordination, which is relatively uncommon among inorganic materials.

INTRODUCTION

Compounds in the system CaO-FeO-Fe_2O_3-Al_2O_3 have been the subject of numerous phase-equilibrium studies. Imlach and Glasser (1971), for example, reported the sub-solidus assemblages at different oxygen partial pressures. Phase relations at liquidus temperatures were studied by the same authors (Imlach and Glasser 1973). This interest is mainly due to the fact that many industrial processes involve these compositions. The relevant materials are Portland cements, high-alumina cements (Taylor 1997), and iron ore sinters (DaCosta and Coheur 1995). In addtion to materials science studies, compounds such as hercynite ($FeAl_2O_4$) and magnetite (Fe_3O_4) are also of geological importance.

Many phases occur on the boundary planes and within the compositional tetrahedron of the CaO-FeO-Fe_2O_3-Al_2O_3 system. However, detailed structural information for compounds within this system containing significant amounts of Fe^{2+} are limited. Spinels like magnetite (Fleet 1981) or hercynite (Larssen et al. 1994) and aenigmatite-type structures such as $Ca_{3.18}Fe^{3+}_{14.66}Al_{1.34}Fe^{2+}_{0.82}O_{28}$ (Mumme et al. 1998) or $Ca_{3.56}Fe^{3+}_{11.91}Al_{4.09}Fe^{2+}_{0.44}O_{28}$ (Arakcheeva et al. 1991) are exceptions. As part of an on-going study on the crystal chemistry of high-pressure calcium aluminates and calcium ferro-aluminates, we obtained and investigated single crystals of a new Fe^{2+}-rich phase in this system. As far as we are aware, this compound represents a previously unknown structure type closely related to spinel but different from the so-called spinelloid phases (e.g., Ross et al. 1992; Woodland and Angel 1998; Angel and Woodland 1998).

EXPERIMENTAL DETAILS

Synthesis and chemical analysis

The starting material for the high-pressure experiments was prepared by solid- state reactions using $CaCO_3$ (Merck, 99%), Al_2O_3 (Aldrich, 99.8%), and Fe_2O_3 (Fluka, 99.9%) in the molar ratio 12:3:1 as reagents. The mixed powders were pressed into pellets and sintered at 1250 °C for 24 h in air. Grinding and firing were repeated twice. The sintered precursor material was reground and used for high-pressure experiments performed at the Bayerisches Geoinstitut. The experiments were carried out in a 1/2 inch piston-cylinder apparatus using talc-pyrex cells with a tapered graphite heater. The samples were encapsulated in 1 cm long and 5 mm diameter welded Pt capsules. The runs were performed at 2.5 GPa and 1250 °C for 48 hours. Pressure was calibrated against the quartz/coesite and kyanite/sillimanite transitions as well as the melting point of diopside. A friction correction of 18% was applied to the nominal pressure on the basis of these calibration data. Temperature was measured with a $Pt_{90}Rh_{10}$-Pt thermocouple and controlled with a Eurotherm 818 controller. Temperatures are considered accurate to within ±10 °C with a temperature gradient of about 5 °C from the top to the middle of the capsule (Shaw and Fliervoet, unpublished data). The experiments were carried out using the hot-piston out technique. The samples were quenched isobarically by turning off the power of the furnace while maintaining pressure within 0.02 GPa of the run pressure. Quench rates were on the order of 75 °C per second. At least two crystalline phases were identified optically in the run product using optical techniques.

Polished single crystals of one of the phases were analyzed

---

* E-mail: vkahlen@zfn.uni-bremen.de

0003-004X/01/1112–1477$05.00

by electron microprobe methods using a CAMECA SX50 instrument in wavelength-dispersive mode. Operating conditions were accelerating potential of 15 kV, probe current of 10 nA, and counting times of 15 s (on peaks). Andradite glass (for Ca and Fe) and pyrope (for Al) were used as primary standards and *K*a lines were used in each case. Elemental concentrations were calculated after matrix correction of the intensity measurements using the ZAF program. Chemical analysis yielded an average composition of 17.97 (±0.15) wt% CaO, 8.64 (±0.09) wt% FeO, and 73.36 (±0.11) wt% Al_2O_3 (total sum = 99.97wt%; numbers in brackets are standard deviations for three crystals and 20 spot analyses each), indicating that Fe in this structure is almost exclusively in the divalent oxidation state. Furthermore, the composition of this crystalline phase is considerably enriched in Al_2O_3 and simultaneously depleted in CaO compared to the bulk composition of the starting material. The formula derived from the chemical analysis based on 32 O atoms is $Ca_{3.95(3)}Fe_{1.48(2)}Al_{17.71(3)}O_{32}$.

Single-crystal structure analysis

X-ray diffraction data were collected on a small (about 140 × 100 × 56 μm), platy, colorless crystal of good optical quality using a Stoe imaging plate single-crystal diffractometer. Parameters of the data collection and of the subsequent structure refinement are summarized in Table 1. An analytical absorption correction based on nine indexed faces was applied. Data reduction included Lorentz and polarization corrections and was performed with the Stoe XRED-software package.

The diffraction symmetry of the crystal was consistent with Laue group 4*/mmm*. Intensity statistics [N(Z)-test and $<E^2 - 1>$] clearly indicated the absence of a center of symmetry. An analysis of the systematically extinct reflections resulted in two possible non-centrosymmetric space groups: $I\bar{4}2d$ and $I4_1md$. The subsequent structure solution confirmed the adequacy of space group choice $I\bar{4}2d$. The crystal structure was solved by a combination of direct methods (SIR92, Altomare et al. 1992) and difference Fourier calculations (SHELXL-93, Sheldrick 1993). The latter program was also used for the least-squares refinements. Drawings of the structure were carried out using the programs ATOMS (Dowty 2000) and ORTEP-3 (Farrugia 1997). X-ray scattering factors for neutral atoms, together with real and imaginary anomalous-dispersion terms, were taken from the *International Tables for X-ray crystallography* (Ibers and Hamilton 1974).

The structure contains three crystallographically different tetrahedral (T) positions and four octahedral (M) sites. The least-squares refinements were started assuming that all octahedral and tetrahedral sites in the structure were occupied by Al only. However, this initial approach resulted in very low displacement parameters for the tetrahedral sites T1 and T2 and for two octahedral positions (M3, M4 in Table 2). As the chemical analysis indicates the presence of Fe in the structure, a model incorporating a random distribution of Fe and Al at these positions was tested.

TABLE 1. Summarized X-ray data collection and refinement parameters

Crystal-cell data	
a	20.1847(14) Å
c	5.6203(6) Å
V	2289.83(3) $Å^3$
Space group	$I\bar{4}2d$
Z	4
Formula	$Ca_4Fe_{1.5}Al_{17.67}O_{32}$
D_{calc}	3.52 g/cm^3
μ	24.13 cm^{-1}
Intensity measurements	
Crystal shape	Fragment of a plate
Crystal dimensions	140 × 100 × 56 mm^3
Diffractometer	Stoe IPDS
Monochromator	Graphite
X-ray radiation	Sealed tube Mo*K*α (0.71073 Å)
X-ray power	50 kV, 40 mA
Θ-range	2.8–28.0°
Reflection range	$\vert h \vert \le 26$; $\vert k \vert \le 26$; $\vert l \vert \le 7$
No. of frames	360
Data collection time per frame	2.5 min.
Rotation width per frame	1°
Measured reflections	10018
Unique reflections in 4*mm*	1389
Observed reflections [$I > 2\sigma(I)$]	1229
R_{int} for 4*mm* (Friedel pairs kept separate)	0.037
Max./min. transmission	0.879/0.803
Refinement of the structure	
Parameters used in the refinement	130
R1 [$F_o > 4\sigma(F_o)$]	0.024
wR2 [$F_o > 4\sigma(F_o)$]	0.060
Weighting parameter a, b	0.038, 0.00
Goodness of Fit	1.068
Final $\Delta\rho_{min}$ ($e/Å^3$)	1.03
Final $\Delta\rho_{max}$ ($e/Å^3$)	–0.47

$R1 = \Sigma \vert\vert F_o\vert - \vert F_c\vert\vert / \Sigma \vert F_o\vert$ $wR2 = [\Sigma(w(F_o^2 - F_c^2)^2] / \Sigma[w(F_o^2)^2)]^{1/2}$

$w = 1 / [\sigma^2(F_o^2) + (aP)^2 + bP]$ $P = [2F_c^2 + max(F_o^2, 0)]/3$

TABLE 2. Fractional atomic coordinates, site occupancies, and equivalent isotropic temperature factors

Atom	Wyckoff-site	Site populations	x	y	z	U(eq)
Ca	16(e)	1.0	0.62758(3)	0.02238(3)	0.1603(1)	0.014(1)
T1	8(d)	0.520(3) Fe 0.480(3) Al	0.70346(4)	¼	⅝	0.011(1)
T2	4(a)	0.093(3) Fe 0.907(3) Al	½	0	¾	0.011(1)
T3	16(e)	1.0 Al	0.61548(5)	0.89541(4)	0.8716(2)	0.009(1)
M1	16(e)	1.0 Al	0.64970(4)	0.17895(4)	0.1285(2)	0.009(1)
M2	8(d)	1.0 Al	¾	0.10496(4)	⅜	0.009(1)
M3	16(e)	0.054(3) Fe 0.946(3) Al	0.74450(4)	0.95239(4)	0.6261(2)	0.010(1)
M4	8(d)	0.076(3) Fe 0.924(3) Al	¾	0.10201(6)	⅞	0.010(1)
O1	16(e)	1.0	0.6860(1)	0.9427(1)	0.3682(5)	0.010(1)
O2	16(e)	1.0	0.7528(1)	0.0441(1)	0.6211(4)	0.010(1)
O3	16(e)	1.0	0.6865(1)	0.9467(1)	0.8822(5)	0.010(1)
O4	16(e)	1.0	0.6158(1)	0.8440(1)	0.1252(5)	0.011(1)
O5	16(e)	1.0	0.6105(1)	0.8482(1)	0.6098(5)	0.012(1)
O6	16(e)	1.0	0.7555(1)	0.1716(1)	0.6279(4)	0.013(1)
O7	16(e)	1.0	0.7480(1)	0.8505(1)	0.6021(4)	0.013(1)
O8	16(e)	1.0	0.5507(1)	0.9514(1)	0.9454(6)	0.016(1)

Notes: *U*(eq) is defined as one third of the trace of the orthogonalized U_{ij} tensor.

No constraints on the bulk chemical composition were applied. However, full occupancy of each site was assumed. The resulting Fe content of 5.94(4) atoms per unit cell agrees well with the electron microprobe analyses. Because the material is likely insulating, formal charges were assigned and in the last cycles, a restraint of 6.0 Fe atoms per cell was introduced in order to achieve charge balance. The final full matrix least-squares calculations using anisostropic displacement parameters yielded a discrepancy index (*R*1) of 0.024. The correct absolute configuration was checked by inspection of the Flack-parameter x = 0.05(4) (Flack 1983). The positional, occupancy and displacement parameters for the structure are given in Tables 2 and 3. Selected interatomic distances and angles as well as distortion parameters of the polyhedra are listed in Table 4. As we did not observe any indications for diffuse streaks or broadening of diffraction spots, the partial site occupancies are not an effect of polytypic stacking disorder.

DESCRIPTION OF THE STRUCTURE

The main building elements of the compound are 11.8 × 7.2 Å wide blocks running parallel to [001] containing $(Fe,Al)O_4$— and $(Fe,Al)O_6$—groups (cf., Fig. 1a). Within a single block, the M3 sites form infinite edge-sharing chains one octahedron wide along *a* or *b*, respectively. A second infinite strip of edge-sharing octahedra with the same width is formed by alternating M2 and M4 sites. The chain direction is along the *c*-axis for the M2/M4 as well as for the M3 strips. The strips are linked by edge-sharing M1 octahedra, and by shared corners with the T3 tetrahedra. Two M1 octahedra form a dimer, the common edge of which is almost parallel to the *c* axis. Furthermore, each single M1 octahedron shares a common edge with one M2 and one M4 as well as two further edges with two different adjacent M3 octahedra. The M2-, M3-, and M4-octahedra have four shared edges each. A drawing of the octahedral sub-lattice is given in Figure 2a. For the different M-sites, all shared octahedral edges are significantly shorter ($<O\text{-}O>_{M1\text{-}M4}$: 2.576 Å) than the unshared ones ($<O\text{-}O>_{M1\text{-}M4}$: 2.782 Å).

The octahedra of a single ribbon enclose a central tunnel

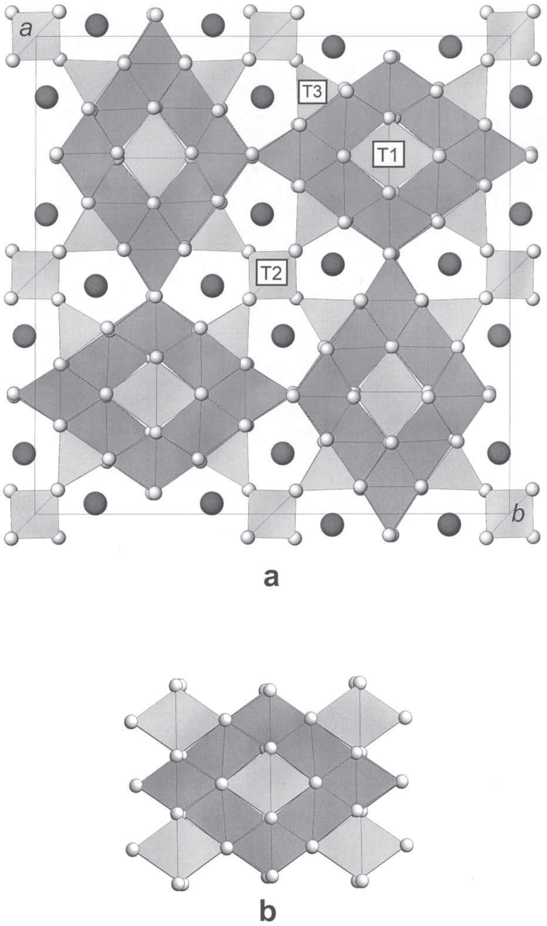

FIGURE 1. **(a)** Projection of the whole crystal structure of $Ca_4Fe_{1.5}Al_{17.67}O_{32}$ parallel to [001]. Spinel-type blocks containing octahedra and tetrahedra are linked by additional T2 tetrahedra and Ca ions (dark grey spheres). **(b)** Corresponding single block cut from the ideal cubic spinel structure.

TABLE 3. Anisotropic displacement parameters $Ca_4Al_{18}FeO_{32}$

Atom	U_{11}	U_{22}	U_{33}	U_{23}	U_{13}	U_{12}
Ca	0.0152(4)	0.0115(3)	0.0152(3)	0.0000(3)	0.0006(2)	0.0014(3)
T1	0.0117(5)	0.0113(5)	0.0103(4)	0.0000(4)	0	0
T2	0.0108(5)	0.0108(5)	0.0112(4)	0	0	0
T3	0.0089(5)	0.0086(5)	0.0089(4)	0.0005(5)	–0.0006(5)	0.0000(4)
M1	0.0092(5)	0.0089(5)	0.0083(4)	0.0005(4)	–0.0002(4)	0.0007(4)
M2	0.0097(7)	0.0089(6)	0.0075(6)	0	0.0010(6)	0
M3	0.0107(5)	0.0105(4)	0.0087(4)	0.0003(4)	–0.0005(5)	–0.0007(4)
M4	0.0104(7)	0.0108(7)	0.0087(2)	0	0.0002(6)	0
O1	0.0102(11)	0.0102(11)	0.0113(11)	–0.0001(11)	–0.0015(11)	–0.0005(8)
O2	0.0105(9)	0.0099(9)	0.0096(9)	–0.0008(9)	–0.0013(14)	0.0004(9)
O3	0.0112(11)	0.0104(11)	0.0102(11)	0.0004(11)	–0.0011(11)	–0.0007(8)
O4	0.0123(11)	0.0114(11)	0.0100(10)	–0.0023(11)	–0.0000(11)	–0.0019(9)
O5	0.0123(11)	0.0132(12)	0.0114(11)	–0.0005(11)	0.0005(10)	–0.0028(9)
O6	0.0121(11)	0.0173(11)	0.0100(10)	–0.0001(10)	0.0018(12)	–0.0045(9)
O7	0.0105(10)	0.0145(10)	0.0133(12)	–0.0031(9)	0.0015(11)	0.0005(11)
O8	0.0136(14)	0.0136(13)	0.0204(11)	–0.0020(13)	–0.0019(13)	0.0017(11)

Notes: The anisotropic displacement factor exponent takes the form: $-2\pi^2 [h^2 a^{*2} U_{11} + ... + 2hka^* b^* U_{12}]$.

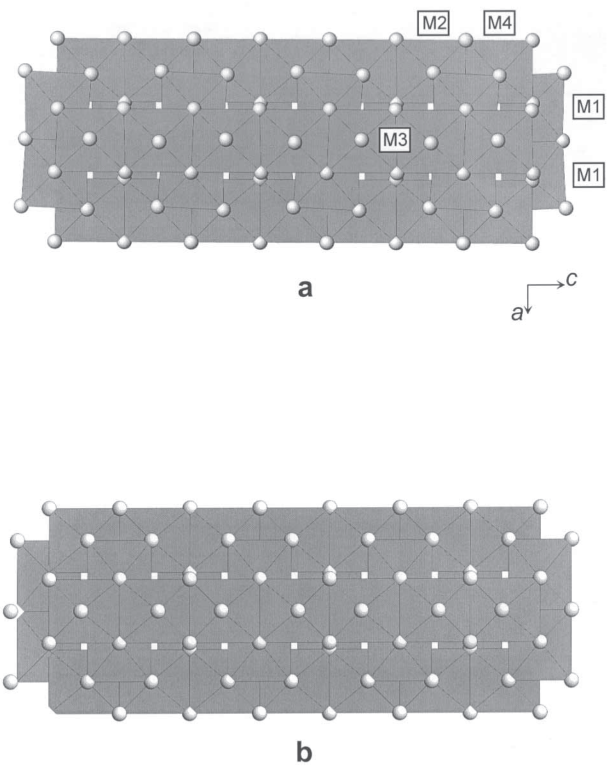

FIGURE 2. **(a)** Sub-structure of the octahedra of the spinel-type block in a projection parellel to [100]. **(b)** Corresponding octahedral substructure in spinel. The distortion of the edges in **(a)** compared to **(b)** is clearly visible.

where the T1 tetrahedra are located. Additional T3-tetrahedra are attached to the outer walls of the blocks. Linkage between adjacent blocks is provided: by (1) T2 tetrahedra residing on the $\bar{4}$-axis, and (2) corner-sharing M3-octahedra belonging to different blocks. The Ca cations reside in the voids between neighboring blocks and are coordinated by seven oxgen ligands. Almost all oxygen atoms are four-coordinated. The only exception is O8, which has three nearest-neighbor cations.

Two different groups of octahedra can be distinguished based upon mean M-O bond distances and polyhedral volumes. The Fe-free octahedra, M1 and M2, have lower values (<M-O>: 1.901 Å) compared to the M3/M4-octahedra (<M-O>: 1.930 Å and 1.938 Å, respectively). Site distortion from spherical symmetry, as measured by quadratic elongation (Q.E.) (Robinson et al. 1997), follows the same trend as site volume, where Q.E.(M1), Q.E.(M2) < Q.E.(M3), Q.E.(M4). Bond valence calculations were performed using the parameters given by Brown and Altermatt (1985) for Al^{3+}-O and Fe^{2+}-O pairs. Assuming that M1 and M2 are exclusively occupied by Al^{3+} yields bond valence sums of 3.01 and 3.02 v.u., respectively. The estimation of the occupation numbers for the disordered sites M3 and M4 based on bond valence calculations results in Al/Fe-ratios of 0.89/0.11 for M4 and 0.93/0.07 for M3, respectively. These estimated values for the Al content are only slightly lower than the results of the structure refinements (cf., Table 4).

The variation in cation distribution among the three tetrahedral sites is also reflected in the T-O bond distances. The smallest site, T3, is Fe free. The mean bond length <T3-O> equals 1.767 Å and is in the normal range observed for AlO_4-tetrahedra. In contrast, substitution of Fe^{2+} for slightly more than one-half of the tetrahedral Al in the T1 site significantly expands the $T(1)O_4$-tetrahedron (Table 4). The average T1-O bond distance of 1.891 Å compares well with the value of 1.892 Å obtained by linear interpolation between 2.012 Å for the $Fe^{2+}O_4$ tetrahedra in spinel-type FeV_2O_4 (Reuter et al. 1969) and 1.767 Å for the Fe-free T3 tetrahedra. The incorporation of a small amount of Fe^{2+} on the T2 site initiates an increase of the mean T-O distance by roughly 1.5% compared to T3. With regard to the deviation from ideal tetrahedral symmetry, there is a consistent site size/distortion relationship: the Q.E. and A.V. values increase in the order T1 < T2 < T3 (cf., Table 4). The comparatively low distortion of the $T(1)O_4$ tetrahedron is a consequence of the location in the center of the tunnels and is imposed by the rigidity of the surrounding octahedral block. In order to rationalize the distortions of the T2- and T3-polyhedra, one must keep in mind the differences in site symmetry. The small amount of Fe^{2+} present in T2 alone cannot explain the significantly lower distortion compared to T3. Furthermore, the differences in the bond valence sums between T3 (BVS: 2.93 v.u.) and T2 (BVS: 2.78 v.u.) would suggest that T2 and not T3 is exposed to a more pronounced tensional strain.

The more regular geometry of the $T(2)O_4$ tetrahedron is due to constraints implied by symmetry (the metal atoms reside on the $\bar{4}$-axis). Inspection of Table 4 reveals that the distortion of the $T(3)O_4$ tetrahedron is mostly limited to bond angles: the values of 119.9(2)° for O5-T3-O8 and 100.8(2)° for O4-T3-O8 represent the extreme values for all observed O-T-O angles in the structure. The distortion is due to cation-cation repulsion between T3 and the neighboring Ca cation across the edge where the small O4-T3-O8 angle occurs. As a compensating effect, the O5-T3-O8 angle on the opposite side opens to a value of about 120°.

The Ca atoms reside in voids between the spinel blocks. The coodination sphere can be approximated by a distorted monocapped trigonal prism (cf., Fig. 3). Actually, Ca shows a (6+1) coordination. The distance of 2.79 Å to the seventh oxygen, O8, is definitely longer compared to the first six anions. However, bond valences around Ca using all seven oxygen atoms are 2.01 v.u., almost equal to its atomic valence.

TABLE 4. Selected interatomic distances (Å), polyhedral distortion indices, and bond angles (°)

T1-O7	1.882(2) × 2	T2-O8	1.793(3) × 4
-O6	1.900(2) × 2		
Mean	1.891	Mean	1.793
V (Å^3)	3.46	V (Å^3)	2.94
Q.E.	1.0013	Q.E.	1.0038
A.V.	4.89	A.V.	15.49
T3-O5	1.756(3)		
-O(4)	1.763(3)		
-O3	1.770(2)		
-O8	1.778(3)		
Mean	1.767		
V (Å^3)	2.78		
Q.E.	1.0120		
A.V.	49.87		
M1-O1	1.870(2)	M3-O3	1.858(3)
-O4	1.886(3)	-O2	1.859(2)
-O7	1.904(3)	-O1	1.879(3)
-O6	1.920(3)	-O3	1.948(3)
-O5	1.925(3)	-O1	1.972(3)
-O7	1.937(3)	-O7	2.062(3)
Mean	1.907	Mean	1.930
V (Å^3)	9.16	V (Å^3)	9.41
Q.E.	1.0062	Q.E.	1.0138
A.V.	21.41	A.V.	43.22
M2-O2	1.851(2) × 2	M4-O2	1.845(2) × 2
-O4	1.910(2) × 2	-O6	1.978(2) × 2
-O6	1.960(2) × 2	-O5	1.991(2) × 2
Mean	1.907	Mean	1.938
V (Å^3)	9.13	V (Å^3)	9.55
Q.E.	1.0091	Q.E.	1.0123
A.V.	29.44	A.V.	39.05
Ca-O4	2.310(2)	-O1	2.312(2)
-O5	2.389(3)	-O8	2.433(3)
-O2	2.460(2)	-O3	2.489(3)
-O8	2.789(3)		
O7-T1-O7	109.2(1)	O8-T2-O8	112.1(1) × 4
O7-T1-O7	110.2(1) × 2	O8-T2-O8	104.4(2) × 2
O7-T1-O6	107.2(1) × 2	Mean	109.5
O7-T1-O6	112.9(1)		
Mean	109.5		
O5-T3-O4	111.0(1)		
O5-T3-O3	113.1(1)		
O5-T3-O8	119.9(2)		
O4-T3-O3	108.3(1)		
O4-T3-O8	100.8(2)		
O3-T3-O8	102.5(1)		
Mean	109.3		

Notes: Q.E. are the quadratic elongations and A.V. the angle variances of the polyhedra as defined by Robinson et al. (1971).

COMPARISON WITH RELATED STRUCTURES

Inorganic compounds having Fe^{2+} in tetrahedral coordination are rare. Two structure families have been already mentioned in the introduction: spinels and aenigmatites. Further examples of structurally characterized compounds are gehlenite type $Ba_2Fe(Ge_2O_7)$ (Malinovskii et al. 1976) and $Fe_2Mo_3O_8$ (Kanazawa and Sasaki 1986).

The comparison between the structure of $Ca_4Fe_{1.5}Al_{17.67}O_{32}$ and spinel shows a close relationship. As can be seen from Figures 2a and 2b, the octahedral substructure of the blocks in $Ca_4Fe_{1.5}Al_{17.67}O_{32}$ can be thought as being cut from the spinel structure with terminating planes parallel to (110), ($1\bar{1}0$), ($\bar{1}10$), and ($\bar{1}\bar{1}0$) (referred to the cubic unit cell). Small differences arise from slight rotations and distortions of the octahedra. Furthermore, the tetrahedra located in the central tunnel of the octahedral unit are the same in both structures (cf., Figs. 1a and 1b).

For tetrahedra attached to the outer walls of the octahedral sub-lattice, the differences are more pronounced. In the spinel structure these rows of tetrahedra are identical to the central tetrahedra, whereas in $Ca_4Fe_{1.5}Al_{17.67}O_{32}$, 50% of these tetrahedra have been removed. The incorporation of Ca cations results in (1) a two-dimensional limitation of the blocks, which extend infinitely parallel to the *c*-axial direction and (2) additonal T2 tetrahedra linking the blocks. No such limitation in space can be found in spinel.

Other structures of geologic interest closely related to the spinel structure type are the so-called spinelloid phases, particularly wadsleyite (b) and ringwoodite (g), which have been implicated in seismic discontinuities and as possible reservoirs for water in the mantle (Smyth 1994). Five different spinelloid polytypes (I-V) have been identified in various systems including Fe_2SiO_4-Fe_3O_4 (Ross et al. 1992; Woodland and Angel 1998;

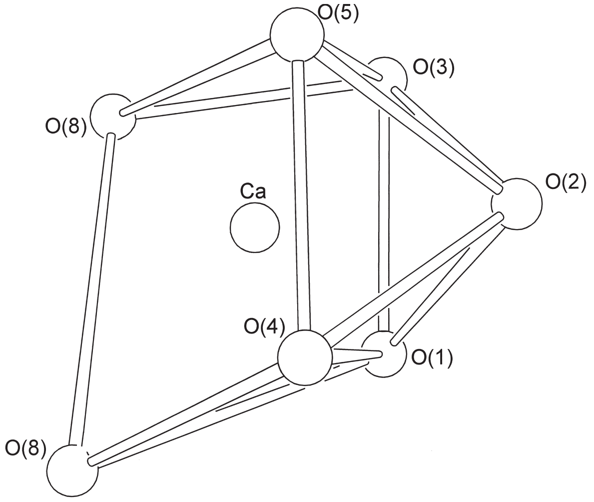

FIGURE 3. Side view of the coordination spheres of the Ca ions in the voids between the blocks.

Angel and Woodland 1998), $NiAl_2O_4$-Ni_2SiO_4 (Ma 1974), $Mg(Ga,Fe)_2O_4$-$MgGe_2O_4$ (Barbier 1989) CoO-As_2O_5 (Barbier 1997). The structural relationships and polytypism among these five types have been discussed by Price (1983). A common feature of the spinelloids and the present compound is the reduced number of tetrahedral sites compared to spinel. However, the spinel-blocks in the spinelloid group still extend in three dimensions. Therefore, the phase discussed in this paper does not belong to the group of spinelloids and as far as we are aware, $Ca_4Fe_{1.5}Al_{17.67}O_{32}$ represents a previously unknown structure type.

ACKNOWLEDGMENTS

J.B.P. is grateful for the support of the NSF, through its EAR program, and for ACS-PRF sponsorship of this work. The manuscript benefited from the helpful comments of two anonymous reviewers.

REFERENCES CITED

Altomare, A., Cascarano, G., Giacovazzo, C., Guagliardi, A., Burla, M.C., Polidori, G., and Camalli, M. (1992) SIR92—a program for automatic solution of structures by direct methods. Journal of Applied Crystallography, 27, 435.

Angel, R.J. and Woodland, A.B. (1998) Crystal structure of spinelloid II in the system Fe_3O_4-Fe_2SiO_4. European Journal of Mineralogy, 10, 607–611.

Arakcheeva, A.V., Karpinskii, O.G., and Lyadova, V.Y. (1991) Crystal structure of aluminum-calcium-ferrite phase with variable composition of the $CaFe_3AlO_7$ type. Soviet Physics Crystallography, 36, 332–336.

Barbier, J. (1989) New spinelloid phases in the $MgGa_2O_4$-$MgGeO_4$ and $MgFe_2O_4$-Mg_2GeO_4 systems. European Journal of Mineralogy, 1, 39–46.

———(1997) $Co_7As_2O_{12}$: a new cobalt arsenate with a spinelloid-type structure. Zeitschrift für Kristallographie, 212, 445–449.

Brown, I.D. and Altermatt, D. (1985) Bond-valence parameters obtained from a systematic analysis of the inorganic crystal structure database. Acta Crystallographica, B41, 244–247.

DaCosta, E. and Coheur, J.P. (1995) Association of calcium ferrites in iron ore sinter with aenigmatites. Ironmaking and Steelmaking, 22, 223–226.

Dowty, E. (2000) ATOMS, Shape Software. Kingsport, TN, U.S.A.

Farrugia, L.J. (1997) ORTEP-3 for Windows. Journal of Applied Crystallography, 30, 565.

Flack, H. (1983) On the enantiomorph-polarity estimation. Acta Crystallographica, A39, 876–881.

Fleet, M.E. (1981) The structure of magnetite. Acta Crystallographica, B37, 917–920.

Ibers, J.A. and Hamilton, W.C., Eds. (1974) International Tables for X-ray crystallography, vol. IV, The Kynoch Press, Birmingham, U.K.

Imlach, J.A. and Glasser, F.P. (1971) Sub-Solidus Relations in the System CaO-Al_2O_3-Fe-Fe_2O_3. Transactions of the British Ceramic Society, 70, 227–234.

———(1973) Phase Relations in the System CaO-Al_2O_3-FeO-Fe_2O_3 at Liquidus Temperatures. Transactions of the British Ceramic Society, 73, 221–228.

Kanazawa, Y. and Sasaki, A. (1986) Structure of Kamiokite. Acta Crystallographica, C42, 9–11.

Larsson, L., O'Neill, H. St.C., Annersten, H. (1994) Crystal chemistry of synthetic hercynite ($FeAl_2O_4$) from XRD structural refinements and Mössbauer spectroscopy. European Journal of Mineralogy, 6, 39–53.

Ma, C.B. (1974) New orthorhombic phases on the join $NiAl_2O_4$-Ni_2SiO_4: stability and implications to mantle petrology. Contributions to Mineralogy and Petrology, 45, 257–279.

Malinovskii, Y.A., Pobedimskaya, E.A., and Belov, N.V. (1976) Synthesis and X-ray analysis of two iron-containing barium germanates $Ba_2Fe(Ge_2O_7)$ and $Fe_2Ba_6Ge_8O_{24}(OH, H_2O)$. Soviet Physics Crystallography, 21, 1195–1197.

Mumme, W.G., Clout, J.M.F., and Gable, R.W. (1998) The crystal stucture of SFCA-I, $Ca_{3.18}Fe^{3+}_{14.66}Al_{1.34}Fe^{2+}_{0.82}O_{28}$, a homologue of the aenigmatite structure type, and new crystal structure refinements of β-CFF, $Ca_{2.99}Fe^{3+}_{14.30}Fe^{2+}_{0.55}O_{25}$ and Mg-free SFCA, $Ca_{2.45}Fe^{3+}_{9.04}Al_{1.74}Fe^{2+}_{0.16}Si_{0.6}O_{20}$. Neues Jahrbuch für Mineralogie Abhandlungen, 173, 93–117.

Price, G.D. (1983) Polytypism and the factors determining the stability of the spinelloid structures. Physics and Chemistry of Minerals, 10, 77–83.

Reuter, B., Riedel, E., Hug, P., Arndt, D., Geisler, U., and Behnke, J. (1969) Zur Kristallchemie der Vanadin(III)—Spinelle. Zeitschrift für Anorganische und Allgemeine Chemie, 369, 306–312.

Robinson, K., Gibbs, V.G., and Ribbe, P.H. (1971) Quadratic elongation: a quantitative measure of distortion in coordination polyhedra. Science, 172, 567–570.

Ross, C.R., Armbruster, T., and Canil, D. (1992) Crystal structure refinement of a spinelloid in the system Fe_3O_4 - Fe_2SiO_4. American Mineralogist, 77, 507–511.

Sheldrick, G.M. (1993) SHELXL-93. A program for the refinement of crystal structures. Universität Göttingen, Germany.

Smyth, J.R. (1994) A crystallographic model for hydrous wadsleyite (β-Mg_2SiO_4): an ocean in the earth's interior. American Mineralogist, 79,1021–1024.

Taylor, H.F.W. (1997) Cement chemistry, Thomas Telford, London, 459 p.

Woodland, A.B. and Angel, R.J. (1998) Crystal structure of a new spinelloid with the wadsleyite structure in the system Fe_2SiO_4-Fe_3O_4 and implications for the Earth's mantle. American Mineralogist, 83, 404–408.

MANUSCRIPT RECEIVED JANUARY 8, 2001
MANUSCRIPT ACCEPTED JULY 18, 2001
MANUSCRIPT HANDLED BY JAMES DOWNS